1997

Relationship between Yeast Polyribosomes and Upf Proteins Required for Nonsense mRNA Decay

Audrey L. Atkin
University of Nebraska-Lincoln, aatkin@unl.edu

Laura R. Schenkman
University of Wisconsin-Madison

Margot Eastham
University of Wisconsin-Madison

Jeffrey N. Dahlseid
University of Wisconsin-Madison

Michael J. Lelivelt
University of Wisconsin-Madison

See next page for additional authors

Published in the *Journal of Biological Chemistry* 272:35 (August 29, 1997), pp. 22163–22172;
doi: 10.1074/jbc.272.35.22163.

Submitted April 11, 1997; revised June 6, 1997.

Relationship between Yeast Polyribosomes and Upf Proteins Required for Nonsense mRNA Decay

Audrey L. Atkin,[1] Laura R. Schenkman,[2] Margot Eastham,[2]

Jeffrey N. Dahlseid,[2] Michael J. Lelivelt,[2] and Michael R. Culbertson[2]

1. School of Biological Sciences, University of Nebraska, Lincoln, Nebraska, USA
2. Laboratories of Genetics and Molecular Biology, University of Wisconsin, Madison, Wisconsin, USA

Corresponding author – Michael R. Culbertson, R. M. Bock Laboratories, 1525 Linden Dr., University of Wisconsin, Madison, WI 53706, telephone 608-262-5388, email mrculber@facstaff.wisc.edu

Abstract

In yeast, the accelerated rate of decay of nonsense mutant mRNAs, called nonsense-mediated mRNA decay, requires three proteins, Upf1p, Upf2p, and Upf3p. Single, double, and triple disruptions of the *UPF* genes had nearly identical effects on nonsense mRNA accumulation, suggesting that the encoded proteins function in a common pathway. We examined the distribution of epitope-tagged versions of Upf proteins by sucrose density gradient fractionation of soluble lysates and found that all three proteins co-distributed with 80 S ribosomal particles and polyribosomes. Treatment of lysates with RNase A caused a coincident collapse of polyribosomes and each Upf protein into fractions containing 80 S ribosomal particles, as expected for proteins that are associated with polyribosomes. Mutations in the cysteine-rich (zinc finger) and RNA helicase domains of Upf1p caused loss of function, but the mutant proteins remained polyribosome-associated. Density gradient profiles for Upf1p were unchanged in the absence of Upf3p, and although similar, were modestly shifted to fractions lighter than those containing polyribosomes in the absence of Upf2p. Upf2p shifted toward heavier polyribosome fractions in the absence of Upf1p and into fractions containing 80 S particles and lighter fractions in the absence of Upf3p. Our results suggest that the association

of Upf2p with polyribosomes typically found in a wild-type strain depends on the presence and opposing effects of Upf1p and Upf3p.

The notion of a global pathway for eukaryotic mRNA decay suggested by early work in animal cells has recently been greatly advanced by studies in the yeast *Saccharomyces cerevisiae* (1–4). Using an *in vivo* transcriptional pulse, the temporal fate of newly synthesized mRNA was established by monitoring poly(A) tail length, loss of the m^7Gppp cap, disappearance of the mRNA, and the appearance of degradation intermediates. mRNAs with shorter half-lives were generally subject to faster rates of deadenylation and decapping. Once the poly(A) tails were reduced to a short oligo(A) length (10–12 nucleotides), the mRNAs were decapped and digested from the 5′ end. Decapping requires Dcp1p (5). Processive degradation from the 5′ end requires the product of the *XRN1* gene, which is known to encode a 5′→3′ exoribonuclease (6). Deadenylation-dependent decapping followed by 5′→3′ exonucleolytic decay is likely to be the global default pathway for the degradation of most eukaryotic mRNAs.

Yeast mRNAs containing a premature stop codon decay more rapidly than their wild-type counterparts (7). This accelerated decay, called nonsense-mediated mRNA decay (NMD),[1] requires cis-acting elements in the mRNA in addition to a premature stop codon (8). Premature translational termination triggers decapping at the 5′ end of nonsense mRNAs with kinetics that are independent of deadenylation (9). Following decapping, decay proceeds through the Xrn1p-mediated nucleolysis that is common to intrinsic decay. These results support the view that when translation is prematurely terminated, the decay of nonsense mRNA is accelerated in part through bypass of a major rate-determining step in the default pathway. This defines NMD as a deadenylation-independent decay pathway.

Three genes, called *UPF1*, *UPF2*, and *UPF3*, encode protein products that are required for NMD in *S. cerevisiae* (10–13). Loss of function of any one of the three genes stabilizes nonsense mRNAs. All three *UPF* genes have been identified, characterized, and sequenced. *UPF1* codes for a 109-kDa protein that contains a cysteine-rich region and an ATPase-helicase domain (10). Purified Upf1p has 5′→3′ RNA/DNA helicase activities and a nucleic acid-dependent ATPase activity (14). Upf1p localizes to the cytoplasm, and the majority of soluble Upf1p is associated with polyribosomes (15). *UPF2* encodes a 126-kDa protein that has a putative nuclear localization sequence and has been implicated in the performance of at least one function in the cytoplasm (11, 12). *UPF3*, which encodes a predominantly nuclear 45-kDa protein (10, 13), contains multiple sequence elements that have recently been shown to promote nuclear import and export across the nuclear envelope.[2] Mutations in Upf3p that are defective for nuclear export confer an Nmd^- phenotype, suggesting that export is connected with the function of Upf3p in NMD.

Physical interactions between the Upf proteins have been studied using the two-hybrid system of Fields and Song (16). A two-hybrid interaction was first detected when *UPF2* was recovered using DNA coding for Upf1p as bait (12). When all possible combinations of the three *UPF* genes were tested for interaction, β-galactosidase activities indicative of strong interactions were detected with the combinations *UPF1-UPF2* and *UPF2-UPF3*.

However, much lower β-galactosidase activity indicative of a weak interaction was revealed when *UPF1* and *UPF3* were combined in two-hybrid test plasmids (17). Genetic evidence was provided suggesting that this weak interaction is indirect and is most likely mediated through Upf2p, which could serve as a bridge between the two proteins. In addition to these interactions, import and export of Upf3p across the nuclear envelope presumably requires docking to nucleoporin receptors that facilitate protein transport through nuclear pores.[2] Taken together, these findings suggest that nuclear and cytoplasmic steps in NMD exist that are functionally linked through interactions between the Upf proteins and the nucleoporins that direct traffic across the nuclear envelope.

In this paper, we have extended our knowledge of the relationships between the Upf proteins using genetic analysis, cell fractionation, and sucrose density gradient fractionation. Single, double, and triple disruptions of the three *UPF* genes confer nonadditive effects on nonsense mRNA accumulation, suggesting that the three proteins act in a common mRNA decay pathway. By analyzing soluble lysates using sucrose density gradient fractionation, we find that Upf1p, Upf2p, and Upf3p all associate with 80 S ribosomal particles and polyribosomes. Mutations in the zinc finger and RNA helicase domains of Upf1p were also analyzed and found to diminish the function of Upf1p in NMD without diminishing the ability of the mutant proteins to associate with polyribosomes. In addition, *UPF* gene disruptions were used to assess whether the typical distribution of Upf1p and Upf2p in sucrose gradients depends on the presence of the other proteins. Our results suggest that the normal association of Upf2p with polyribosomes depends on the presence and opposing effects of the other two proteins. Also, we report that quantitative measurements of the relative cellular protein concentrations of Upf1p and Upf3p indicate a lack of 1:1 stoichiometry. The implications of these findings are discussed in the context of the cellular distribution, physical interactions, and functional relationships between the three proteins.

Experimental Procedures

Strains, Plasmids, and Genetic Methods

Strains of *S. cerevisiae* and plasmids are listed in Tables I and II, respectively. Yeast strains were constructed, grown, and maintained using standard techniques (18). Yeast transformations were performed using the LiAc method (19) or by electroporation (20). *Escherichia coli* strain DH5α was used for preparation of plasmid DNAs. Methods for growth, maintenance, and transformation of bacteria are described by Sambrook et al. (21). Plasmid DNAs were prepared from *E. coli* using a QIAprep spin plasmid miniprep kit (Qiagen Inc., Chatsworth, CA) or by the method of Lee and Rasheed (22).

To test the effects of multiple *UPF* gene disruptions on nonsense mRNA accumulation, strain LRSY307 (Table I) was constructed. LRSY307 carries three marked disruption alleles, *upf1::ura3*2, *upf2::HIS3*, and *upf3::TRP1*. Wild-type *UPF1*, *UPF2*, or *UPF3* genes were transformed into LRSY307 in all possible combinations on *URA3 CEN6* or *LEU2 CEN6* plasmids (Table II), resulting in an isogenic set of strains that collectively represent all possible single, double, and triple disruptions. To measure the effects of the *upf1–3* and *UPF1-D4* mutations on NMD, isogenic strains were constructed using strain PLY38 (Table I). PLY38

contains *upf1–2*, which confers complete loss of function (10). Plasmids carrying *upf1–3* and *UPF1-D4* were transformed into PLY38 on *URA3 CEN6* plasmids (Table II).

Table I. Yeast strains

Strain	Genotype
AAY181	*MAT*a *upf1-Δ1::URA3 upf3-Δ1::TRP1 ura3–52 trp1–7 leu2–3,112*
LRSY21	*MATα his4–38 SUF1–1 ura3–52 upf2–1*
LRSY203	*MATα trp1-Δ1 his4–38 SUF1–1 upf3-Δ1::TRP1 ura3–52 leu2–3*
LRSY307	*MAT*a *his3–11,15 ura3–52 trp1-Δ1 leu2 upf1-Δ2::ura3-upf2-Δ1::HIS3 upf3-Δ1::TRP1*
JDY8	*MATα leu2–3,112 trp1-Δ1 ura3–52 his3–11,-15 upf2-Δ1::HIS3*
PLY102	*MAT*a *upf1-Δ1::URA3 ura3–52 trp1–7 leu2–3,112*
PLY38	*MAT upf1–2 his4–38 SUF1–1 ura3–52*
YJP121	*MATa ura3–52 lys2–801 ade2–101 his3-Δ200 trp1-Δ63 leu2-Δ1 upf2-Δ1::HIS3*

Note: All strains were constructed for this study except PLY102 and PLY38, which were described previously (7). YJP121 was obtained from P. Hieter.

Table II. Plasmids

Plasmid	Vector	Yeast genes
pRS315		*LEU2 CEN6 ARS4*
pRS316		*URA3 CEN6 ARS4*
pRS315UPF1	pRS315	*LEU2 CEN6 ARS4 UPF1*
pRS316UPF1	pRS316	*URA3 CEN6 ARS4 UPF1*
pRS316upf1–3	pRS316	*URA3 CEN6 ARS4 upf1–3*
pRS316UPF1-D4	pRS316	*URA3 CEN6 ARS4 UPF1-D4*
pRS315UPF1–3HA	pRS315	*LEU2 CEN6 ARS4 UPF1–3HA*
pRS314UPF1–3HA	pRS314	*TRP1 CEN6 ARS4 UPF1–3HA*
pRS314UPF1-D4–3HA	pRS314	*TRP1 CEN6 ARS4 UPF1-D4–3HA*
pRS314upf1–3-3HA	pRS314	*TRP1 CEN6 ARS4 upf1–3-3HA*
pUZ178	pRS316	*URA3 CEN6 ARS4 UPF2*
pRS316UPF2–3myc	pRS316	*URA3 CEN6 ARS4 UPF2–3myc*
pLS17	pRS316	*URA3 CEN6 ARS4 UPF3*
pLS51	pRS316	*URA3 CEN6 ARS4 UPF3–3HA*
pLS74	pRS315	*LEU2 CEN6 ARS4 UPF3*
pLS80	pRS316	*URA3 CEN6 ARS4 UPF1 UPF2*

Note: All plasmids were constructed for this study or were described previously (15) except pUZ178, which was obtained from P. Hieter.

RNA Methods

Yeast total RNA was isolated by hot phenol extraction (7). For Northern blotting, RNA samples were denatured either by treatment with glyoxal and Me_2SO or formamide-formaldehyde before fractionation on 1.0% agarose gels (23) or 1.0% agarose, 16.2% formaldehyde gels (15). Gels were loaded with 10 mg of total RNA per lane. Fractionated RNAs were transferred to GeneScreen Plus membranes (NEN Life Science Products). DNA probes were prepared from restriction fragments or polymerase chain reaction fragments

as described by Atkin et al. (15). Hybridization of DNA probes to RNA blots was essentially as described by Klessig and Berry (24).

Construction of UPF Alleles Coding for Epitope-tagged Proteins

The *UPF1–3EP* allele encodes a functional, epitope-tagged version of Upf1p that contains three tandem copies of the influenza virus hemagglutinin (HA) protein epitope immediately adjacent to the last amino acid of Upf1p as described previously (15). The HA epitopes are recognized by monoclonal antibody (mAb) 12CA5. In this paper, we refer to the modified gene and protein as *UPF1–3HA* and Upf1p-3HA, respectively.

UPF2 was modified by placing a DNA sequence encoding three copies of a c-Myc epitope immediately upstream of the translation termination codon to create *UPF2–3myc*. A 1110-base pair *Eco*RI-*Hin*cII fragment from the 3′ end of *UPF2* was subcloned into the *Eco*RI-*Sma*I sites of pBKCMV (Stratagene, La Jolla, CA). The sequence 5′-CGT AGT TTC GAC TTG GGC CCA TGA-3′, which contains a unique *Bsp*120I site, was inserted at the *Psp*1406I site near the *UPF2* stop codon, resulting in loss of the *Psp*1406I site. A *Not*I fragment coding for three copies of the c-Myc epitope was cloned into the *Bsp*120I site. An *Eco*RI-*Kpn*I fragment containing the c-Myc epitopes was used to replace the same region of a wild-type *UPF2* gene carried on pRS316, resulting in plasmid pRS316UPF2–3myc (Table II). Using 9E10 mAbs, the tagged protein, Upf2p-3myc, was detected on Western blots as a 130-kDa protein whose appearance is unique to strains carrying the modified gene.

UPF3 was modified by placing a DNA sequence encoding three tandem copies of the HA epitope between the fourth and fifth codons near the 5′ end to create *UPF3–3HA*. Annealed oligodeoxynucleotides (5′-TGC GGC CGC TCT AGA AGC GGC CTC TTG-3′ and 5′-AGC GGC CGC TTC TAG AGC GGC CGC ACA-3′), carrying *Not*I and *Xba*I sites were introduced into the *Bsr*DI site near the 5′ end of *UPF3*. A *Not*I DNA fragment encoding three tandem copies of the HA epitope was inserted into the *Not*I site, resulting in plasmid pLS51 (Table II). Using 12CA5 mAbs, the tagged protein, Upf3p-3HA, was detected on Western blots as a 49-kDa protein whose appearance is unique to strains carrying the modified gene.

Construction of Mutant Alleles of UPF1

The mutation *upf1–3* is a substitution of serine for cysteine at position 122, which is located in the zinc finger region of *UPF1* (25). We constructed this allele using two polymerase chain reaction products amplified in separate reactions with primer pair UPF1wt352a (5′-TAT CCC CTA AGT CAG AAT CTG G-3′) and ALA1wt (5′-GAT TTC ATC AGG AAA GAA GGA AGG GCA G-3′) and primer pair UPF1MUT1s (5′-CCG TTT TGG AAT CTT ATA ACT GTG-3′) and mutagen B (5′-GTG TTG GAG GTG GCG TTT TAC T-3′). Polymerase chain reaction products were blunt-ended with T4 DNA polymerase, ligated, and digested with *Bst*XI and *Sph*I. Fragments of the correct size were gel-purified, subcloned into pBluescript (Stratagene), and analyzed by DNA sequence analysis. *Bst*XI/*Eco*RV fragments carrying the Ser^{122} mutation were used to replace a *Bst*XI/*Eco*RV DNA fragment in the wild-type *UPF1* gene and the *UPF1–3HA* gene to produce *upf1–3* and *upf1–3-3HA*. These genes are carried on the plasmids pRS316upf1–3 and pRS314upf1–3-3HA, respectively (Table II).

The mutation *UPF1-D4*, described previously (10), causes a substitution of arginine for cysteine at position 779, which is located at a conserved position in the RNA helicase domain. The mutant allele is carried on plasmid pRS316UPF1-D4 (Table II). A modified gene was constructed that codes for the protein Upf1-D4p-3HA, which contains the *D4* mutation plus a triple HA tag at the C terminus. This was accomplished by replacing a *Nru*I-*Bam*HI fragment at the 3′ end of *UPF1-D4* with a *Nru*I-*Bam*HI fragment from *UPF1–3HA*, resulting in the plasmid pRS314UPF1-D4–3HA (Table II).

Functional Assays for Epitope-tagged Upf Proteins

Epitope-tagged proteins were assayed for function by growth tests in strains lacking the corresponding wild-type gene using a previously described allosuppression assay (10). Strains carrying wild-type *UPF* genes, the frameshift mutation *his4–38*, and the tRNA frameshift suppressor *SUF1–1* produce an unstable his4–38 mRNA, resulting in failure to grow at 37°C on medium lacking histidine. Impaired function of any one of the three Upf proteins stabilizes the mRNA, resulting in growth on medium lacking histidine at 37°C. Centromeric plasmids carrying *UPF2–3myc* or *UPF3–3HA* were transformed into strains lacking the corresponding wild-type *UPF* gene and carrying *his4–38* and *SUF1–1*. Using the allosuppression assay, we showed previously that the strain carrying *UPF1-HA* (formerly *UPF1–3EP*) grew poorly on medium lacking histidine at 37°C (15), suggesting that function was retained. Quantitative measurement of his4–38 mRNA levels by Northern blotting showed that Upf1p-3HA retained 80–90% of function compared with the wild-type protein. Growth tests using strains carrying *UPF2–3myc* and *UPF3–3HA* gave similar results, indicating the all three of the tagged proteins retain function at a level comparable with wild type. The stabilities of the tagged proteins are therefore presumed to be similar to the corresponding wild-type proteins.

Protein Extraction, Fractionation, and Detection

The relative abundance and solubility of epitope-tagged proteins was determined by fractionation of total proteins from cell lysates. Yeast cultures were grown to an A_{600} of 0.4–0.6. Half of the culture was extracted with a total protein lysis buffer (5 mM EDTA, 250 mM NaCl, 0.1% Nonidet P-40, 50 mM Tris-HCl, pH 7.4), while the other half was extracted with polyribosome lysis buffer (100 mM NaCl, 33 mM $MgCl_2$, 0.1% diethyl pyrocarbonate, 50 mM cycloheximide, 0.2 mg/ml heparin, 10 mM Tris-HCl, pH 7.5). Soluble extracts were quantified using a BCA protein concentration kit (Pierce). A concentrated 4 × Laemmli buffer was added to both soluble extracts to a 1 × final concentration. The insoluble material remaining after the lysis buffer extractions was further extracted with 1 × Laemmli buffer. The presence of the reducing agents in 1 × Laemmli buffer, which are necessary for efficient solubilization, interfered with accurate protein quantification. To circumvent this, the volume of 1 × Laemmli buffer used in the second extraction was equal to the final adjusted volume of the respective soluble extract. We reasoned that using equal volumes from both the first and second extractions would provide equivalent representative samples from each extraction. Using these equivalent representative samples allows for a direct comparison of the relative amount of a given protein present in each extraction.

For a given lysis buffer, a known amount of protein from the first extraction and an equal volume, and therefore an equivalent representative sample, from the second extraction were fractionated by SDS-polyacrylamide gel electrophoresis. The proteins were transferred to Immobilon-NC membranes (Millipore Corp., Bedford, MA) and examined by quantitative Western blotting. Upf1p-3HA and Upf3p-3HA were detected with 12CA5 mAbs (Berkeley Antibody Company, Richmond, CA), and Upf2p-3myc was detected with 9E10 mAbs (Hybridoma Facility, University of Wisconsin Biotechnology Center, Madison, WI). ^{35}S-Labeled secondary antibodies specific for mouse Ig (Amersham Life Sciences) were used at a concentration of 0.1 μCi/ml.

For sucrose density gradient fractionation, proteins were extracted in polyribosome lysis buffer and fractionated on 7–47% sucrose gradients prepared as described previously (15). Upf1p-3HA, Upf2p-3myc, and Upf3p-3HA were detected in sucrose gradient fractions by Western blotting using ECL and Hyperfilm (Amersham Life Sciences) as described previously (14). Films of the Western blots were analyzed with a Molecular Dynamics densitometer (Sunnyvale, CA).

Results

UPF Genes Function in a Common mRNA Decay Pathway

CYH2 pre-mRNA accumulation has been shown to be a sensitive indicator of whether the NMD pathway is functional (26). *CYH2*, which encodes the ribosomal protein L29, contains an intron that is inefficiently spliced. An in-frame premature termination codon located within the intron targets the CYH2 pre-mRNA for accelerated decay (27). To assess the effects of multiple *upf* mutations on NMD, we determined the degree to which CYH2 pre-mRNA accumulates relative to the mature CYH2 mRNA by Northern blotting of total RNA from isogenic derivatives of strain LRSY307 (Table I). Collectively, these strains represent all possible combinations of triple, double, and single null alleles of *UPF1*, *UPF2*, and *UPF3* (see "Experimental Procedures"; Table I).

Northern blots were probed with a labeled DNA fragment corresponding to nucleotides 15–780 of the CYH2 ORF and intron (27). The CYH2 pre-mRNA/mRNA accumulation ratios were determined and used to calculate the relative accumulation of CYH2 pre-mRNA (Table III). For strains carrying the single, double, or triple disruptions, the relative accumulation of CYH2 pre-mRNA ranged from 3.2 to 3.8 (average 3.4). These results indicate that the effects of double and triple disruptions on CYH2 pre-mRNA accumulation are nonadditive compared with the effects of single gene disruptions, suggesting that all three *UPF* genes function in a common mRNA decay pathway.

Table III. Accumulation of CYH2 pre-mRNA in strains carrying upf null alleles

Plasmids in strain LRSY307	Genotype	Accumulation ratio	Relative accumulation
pUZ178, pLS74	*upf1—*	1.9 (0.26)	3.2
pRS316UPF1, pLS74	*upf2—*	2.1 (0.04)	3.5
pLS80, pRS315	*upf3—*	2.0 (0.01)	3.3
pRS316, pLS74	*upf1—, upf2—*	2.0 (0.19)	3.3
pRS316UPF1, pRS315	*upf2—, upf3—*	2.1 (0.00)	3.5
pUZ178, pRS315	*upf1—, upf3—*	2.3 (0.46)	3.8
pRS316, pRS315	*upf1—, upf2—, upf3—*	2.0 (0.10)	3.3
pLS80, pLS74	*UPF1, UPF2, UPF3*	0.6 (0.00)	1.0

Note: CYH2 pre-mRNA/CYH2-mRNA accumulation ratios were determined by quantitative Northern blotting. Relative accumulation for each strain was calculated by dividing the pre-mRNA/mRNA accumulation ratio by the ratio established for the strain carrying wild-type *UPF1*, *UPF2*, and *UPF3*. S.D. values are shown in parentheses (n = 2). Strain LRSY307 is described in Table I, and the plasmids are described in Table II.

Solubility and Relative Abundance of Upf Proteins

To evaluate the results of the sucrose gradients presented below, we determined the solubility and relative abundance of epitope-tagged Upf proteins by quantitative Western blotting. Cell extracts were prepared from strains PLY102[pRS314UPF1–3HA], JDY8[pRS316UPF2–3myc], and LRSY203[pLS51 (*UPF3–3HA*)] (Tables I and II). The plasmids in these strains contain the genes coding for Upf1p-3HA, Upf2p-3myc, and Upf3p-3HA. Cell lysates were prepared using two different lysis buffers, one containing 100 mM NaCl (polyribosome lysis buffer) and the other containing 250 mM NaCl and 0.1% Nonidet P-40 detergent (total protein lysis buffer) (see "Experimental Procedures").

The relative amounts of each of the three proteins extracted were quantified using ^{35}S-labeled secondary antibodies on Western blots by PhosphorImager (Molecular Dynamics) analysis (Fig. 1). To compare the relative efficiencies of extraction for each lysis buffer, we calculated the percentage of Upf protein extracted with each lysis buffer (Fig. 1, *lane 1* or *3*) relative to the sum of total protein extracted (Fig. 1, either *lanes 1* plus *2* or *lanes 3* plus *4*). We found that 64, 58, and 40% of total Upf1p-3HA, Upf2p-3myc, and Upf3p-3HA, respectively, were soluble in the total protein lysis buffer (Fig. 1, Table IV). In polyribosome lysis buffer, 44, 24, and 15% of total Upf1p-3HA, Upf2p-3myc, and Upf3p-3HA, respectively, were soluble (Fig. 1, Table IV). These results indicate that a significant portion of each of the three proteins is soluble in the polyribosome lysis buffer. However, since polyribosome lysis buffer did not completely solubilize the Upf proteins, the sucrose gradients represent an analysis of the distribution of only the soluble fraction for each protein.

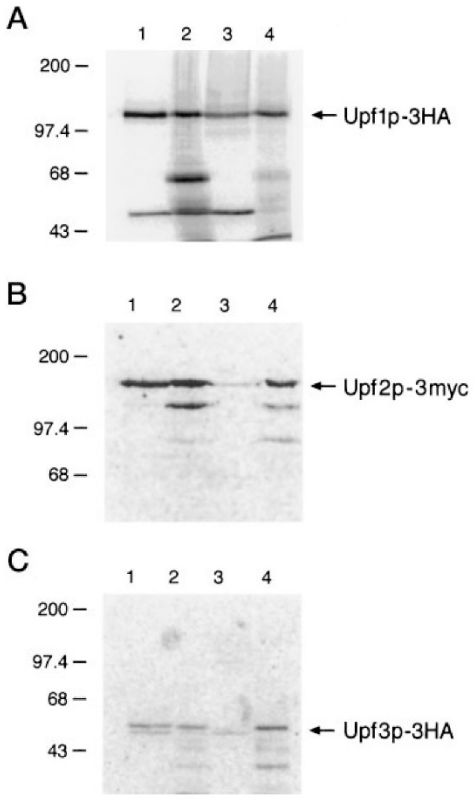

Figure 1. Differential extraction of Upf1p-3HA, Upf2p-3myc, and Upf3p-3HA. The figure shows ^{35}S-labeled Western blots of cell extracts prepared from strain PLY102[pRS314UPF1–3HA] (A), strain JDY8[pRS316UPF2–3myc] (B), and LRSY203[pLS51], which carries Upf3p-3HA (C). Cells were extracted with a total protein lysis buffer (*lane 1*) or polyribosome lysis buffer (*lane 3*) (see "Experimental Procedures"). The pellets of insoluble material from lysis buffer extractions were extracted with 1 × Laemmli buffer (*lanes 2* and *4*). Equal volumes from adjusted lysis buffer and Laemmli buffer extractions were resolved by 7.5% SDS-polyacrylamide gel electrophoresis (Upf1p-3HA and Upf2p-3myc) or 10% SDS-polyacrylamide gel electrophoresis (Upf3p-3HA and control). Upf1p-3HA and Upf3p-3HA were detected with 12CA5 mAbs, and Upf2p-3myc was detected with 9E10 mAbs on Western blots. The primary mAbs were detected with ^{35}S-labeled secondary antibodies specific for mouse Ig. The positions of bands in a prestained set of molecular weight standards are indicated to the left in each panel. Exposures of the Western blots were individually optimized and do not visually reflect the stoichiometric difference between Upf1p and Upf3p.

Table IV. Differential solubility of epitope-tagged Upf proteins

	Total protein lysis buffer		Polyribosome lysis buffer	
Protein	Buffer	Pellet	Buffer	Pellet
Upf1p-3HA	64 ± 0%	36 ± 0%	44 ± 4%	56 ± 4%
Upf2p-3myc	58 ± 5%	42 ± 5%	24 ± 5%	76 ± 5%
Upf3p-3HA	40 ± 6%	60 ± 6%	15 ± 1%	85 ± 1%

Note: S.E. is reported as a measure of the variation observed on two trials.

The epitope-tagged versions of Upf1p and Upf3p contain the same triple HA epitope. The amounts of each protein were compared to estimate the stoichiometric relationship between the two. We calculated the relative protein ratio from the sum of Upf1p-3HA detected in *lanes 1* and *2* (Fig. 1) compared with the same sum for Upf3p-3HA. The ratio was corrected for differences in total protein loaded from the lysis buffer fractions. Using this approach, we found that Upf1p-3HA is 66-fold more abundant than Upf3p-3HA. Assuming this reflects a difference in the *in vivo* concentrations of the two proteins, this result suggests that Upf1p and Upf3p are not present at 1:1 stoichiometry.

Distribution of Upf1p-3HA in Strains Carrying Gene Disruptions in UPF2 and UPF3

Previously, we showed that Upf1p-3HA codistributes with both polyribosomes and the ribosomal protein L1 of the 60 S ribosomal subunit by sucrose gradient fractionation (15). Upf1p-3HA coshifted along with L1 into fractions coincident with 80 S particles when growth conditions were altered or when polyribosomes were disrupted by treatment with RNase A. These results suggested an association between Upf1p-3HA and polyribosomes. In this study, we examined whether the distribution of Upf1p-3HA depends on the presence of Upf2p or Upf3p.

First, a soluble lysate was prepared from strain PLY102[pRS315UPF1–3HA], which carries the wild-type alleles of *UPF2* and *UPF3* (Tables I and II). Proteins were fractionated in a sucrose gradient, and the distribution of Upf1p-3HA was determined by ECL Western blotting (Fig. 2). Although ECL provides a nonlinear reflection of protein abundance, useful comparisons can still be made by examining the relative overall pattern of protein distribution across the gradient. Using this approach, Upf1p-3HA was found to be distributed throughout the sucrose gradient (Fig. 2A). The majority was detected in fractions 10–24, which also contain 40 and 60 S subunits, 80 S ribosomal particles, and polyribosomes. There was a peak of accumulation in fractions 13–15, the same fractions that contain the 80 S ribosomal particles. Some Upf1p-3HA also accumulated in low density fractions, where monomeric proteins and small complexes migrate.

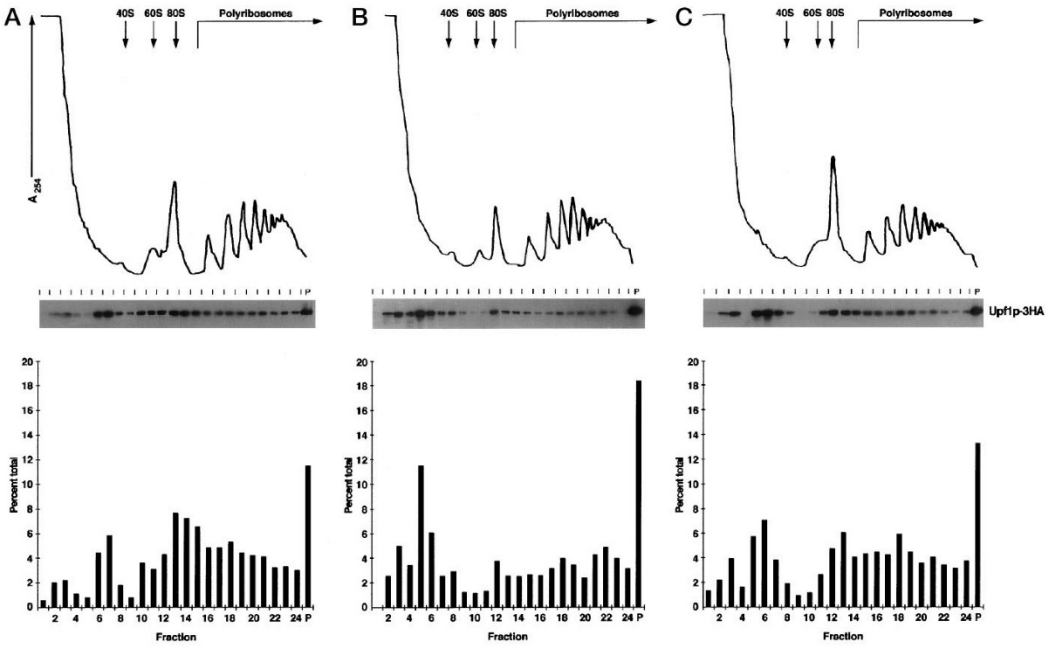

Figure 2. 7–47% sucrose density gradient fractionation of Upf1p-3HA in the presence or absence of a functional *UPF2* or *UPF3* gene. Cell extracts were prepared from strain PLY102[pRS315UPF1–3HA] (A), which carries functional versions of all three *UPF* genes, strain YJP121[pRS315UPF1–3HA] (B), which carries a *UPF2* disruption, and strain AAY181[pRS315UPF1–3HA] (C), which carries a UPF3 disruption. Absorbance at A_{254} was monitored across the gradient to locate fractions containing 40 and 60 S ribosomal subunits, 80 S ribosomal particles, and polyribosomes. The proteins were recovered by acetone precipitation, resolved by 10% SDS-polyacrylamide gel electrophoresis, and detected by ECL Western blotting. Solubilized pellets from the sucrose gradients (*P*) were included on the right of the Western blots.

To monitor the effects of disrupting *UPF2* on the distribution of Upf1p-3HA, we compared the distribution in Figure 2A with that obtained using strain YJP121[pRS315UPF1–3HA] (Fig. 2B), which contains the *UPF1–3HA* gene and a disruption of *UPF2* (Tables I and II). Upf1p-3HA was distributed throughout the gradient with the majority detected in fractions 12–24 and the remainder in fractions near the top of the gradient. Comparison of the histograms in Figure 2, A and B, indicates that a minor amount of Upf1p-3HA shifts from polyribosome fractions to lighter fractions in the absence of Upf2p, but a significant amount of Upf1p-3HA remains in the fractions containing polyribosomes. This suggests that Upf1p can still associate with polyribosomes when *UPF2* is disrupted.

A similar approach was used to assess how a disruption of the *UPF3* gene affects the distribution of Upf1p-3HA using strain AAY181[pRS315UPF1–3HA] (Tables I and II), which contains the *UPF1–3HA* gene and a disruption of *UPF3*. Upf1p-3HA was again distributed throughout the gradient in a pattern resembling that found for strain PLY102[pRS315UPF1–3HA] (Fig. 2C). The results seen in Figure 2, A and C, were similar,

indicating that the previously demonstrated association of Upf1p with polyribosomes does not depend on the presence of Upf3p.

Effects of Mutations in the Cysteine-rich Region and the Helicase Domain of Upf1p

We analyzed additional mutations in *UPF1* that were deemed of special interest because of their previously described biochemical or genetic properties (10, 25). One mutation, *upf1–3*, is a substitution of serine for cysteine in a region of the protein that contains multiple cysteine residues that could be involved in binding zinc (Fig. 3). This mutation causes reduced RNA helicase activity and impaired physical interaction with Upf2p (25). Another mutation, *UPF1-D4*, is located in the helicase domain. This mutation causes dosage-dependent, dominant-negative inhibition of wild-type Upf1p function (10).

Both of these mutations were examined to determine the extent to which they impair Upf1p function and whether they cause any change in the distribution of Upf1p in sucrose gradients. The function of Upf1p was assayed by allosuppression in strains carrying the mutations (see "Experimental Procedures"). This assay monitors the extent of growth proportional to accumulation of his4–38 mRNA. Both of the mutations conferred growth at 37°C in media lacking histidine that was comparable with growth conferred by the null allele *upf1–2* (Fig. 3B). These results indicate that *upf1–3* and *UPF1-D4* significantly impair the function of Upf1p.

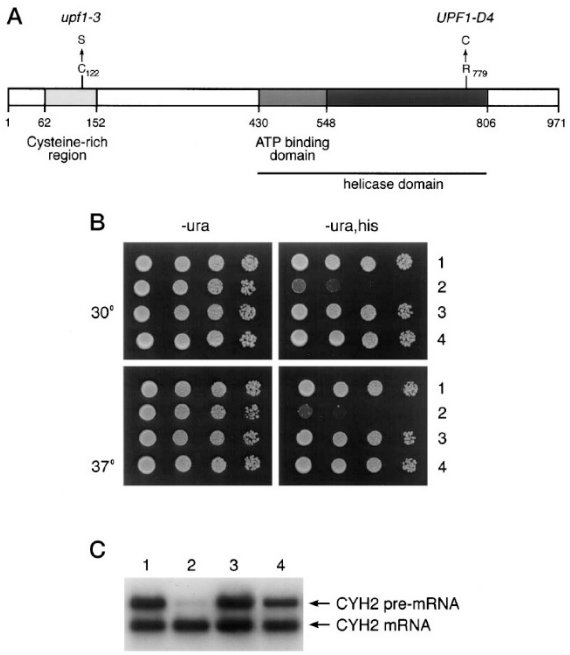

Figure 3. Characterization of mutant alleles of *UPF1*. A, location and nature of mutations in *UPF1*. The relevant wildtype amino acid sequence is shown immediately above the schematic diagram of Upf1p. *Subscript numbers* indicate the positions of the amino acids. *Arrows* denote the location of the mutations and the resulting amino acid change. B, growth tests using an allosuppression assay (see "Experimental Procedures") to assess

the ability of the mutant *UPF1* alleles to compensate for loss of wild-type *UPF1* function. Strain PLY38 was separately transformed with pRS316 (1), pRS316UPF1 (2), pRS316upf1–3 (3), and pRS316UPF-1-D4 (4). Growth of the transformants was tested by plating 10^0, 10^{-1}, 10^{-2}, and 10^{-3} serial dilutions of log phase cultures (*left* to *right*) onto –uracil, and –uracil–histidine plates at 30°C and at 37°C. C, effect of mutations on the accumulation of CYH2 pre-mRNA. An autoradiograph of a representative Northern blot is shown. Northern blots were prepared using total RNA isolated from strain PLY38 separately transformed as described for panel B. The Northern blots were probed with a DNA fragment complementary to nucleotides 15–780 of the *CYH2* ORF and intron (27).

We also assessed the effects of the mutations on the accumulation of CYH2 pre-mRNA. Total RNA from each mutant strain was analyzed by Northern blotting using a probe specific for CYH2 RNA. The relative accumulation of CYH2 pre-mRNA was compared with the relative accumulation in the wild-type strain and the strain carrying the *upf1–2* null allele (Fig. 3C). From the relative accumulation, we calculated (see Table V legend) that *upf1–3* retained only 15% of function compared with wild type and thus approaches complete loss of function. *UPF1-D4* retained 62% of function in the absence of wild-type *UPF1*. Thus, although *UPF1-D4* causes loss of function as measured by allosuppression, pre-CYH2 accumulation indicates that the function of the mutant protein is only partially diminished.

Table V. Accumulation of CYH2 pre-mRNA in strains carrying upf1–3 and UPF1-D4

Plasmid in strain PLY38	Genotype	Accumulation ratio	Relative accumulation	Function retained (%)
pRS316	*upf1–2*	1.5 (0.21)	7.5	0
pRS316UPF1	*UPF1*	0.2 (0.64)	1.0	100
pRS316upf1–3	*upf1–3*	1.3 (0.01)	6.5	15
pRS316UPF1-D4	*UPF1-D4*	0.7 (0.01)	3.5	62

Note: CYH2 pre-mRNA:CYH2-mRNA accumulation ratios were determined by quantitative Northern blotting. Relative accumulation for each strain was calculated by dividing the pre-mRNA:mRNA accumulation ratio by the ratio established for strain PLY38[pRS316UPF1]. The *upf1–2* mutation in strain PLY38[pRS316] confers complete loss of function (10). The percentage of function retained for *upf1–3* and *UPF1-D4* was calculated from the accumulation ratios and is equal to $1 - ((\text{ratio}_{upf1\text{–}3\ (\text{or } UPF1\text{-}D4)} - \text{ratio}_{UPF1})/(\text{ratio}_{upf1\text{–}2} - \text{ratio}_{UPF1})) \times 100$. S.D. values are shown in parentheses ($n = 2$).

We compared the distribution of the mutant proteins with that of wild-type Upf1p in sucrose gradients. For this purpose, mutant alleles were constructed that code for the epitope-tagged mutant proteins Upf1–3p-3HA and Upf1-D4p-3HA (see "Experimental Procedures"). Soluble lysates were prepared and analyzed from the strains PLY102[pRS314UPF1–3HA], PLY102[pRS314upf1–3-3HA], and PLY102[pRS314 UPF1-D4–3HA] (Fig. 4, A, B, and C, respectively). Upf1p-3HA and Upf1–3p-3HA were both distributed throughout the gradient with similar peaks of accumulation both in fractions containing polyribosomes and in lighter fractions. Unlike these two proteins, very little Upf1-D4p-3HA was detected in the lightest fractions (Fig. 4C, fractions 1–5). Most of the protein

was detected in peak fractions corresponding to 80 S ribosomal particles and polyribosomes (fractions 9–24). Assuming no change in protein stability, this suggests that the mutation may cause a modest shift to heavier fractions.

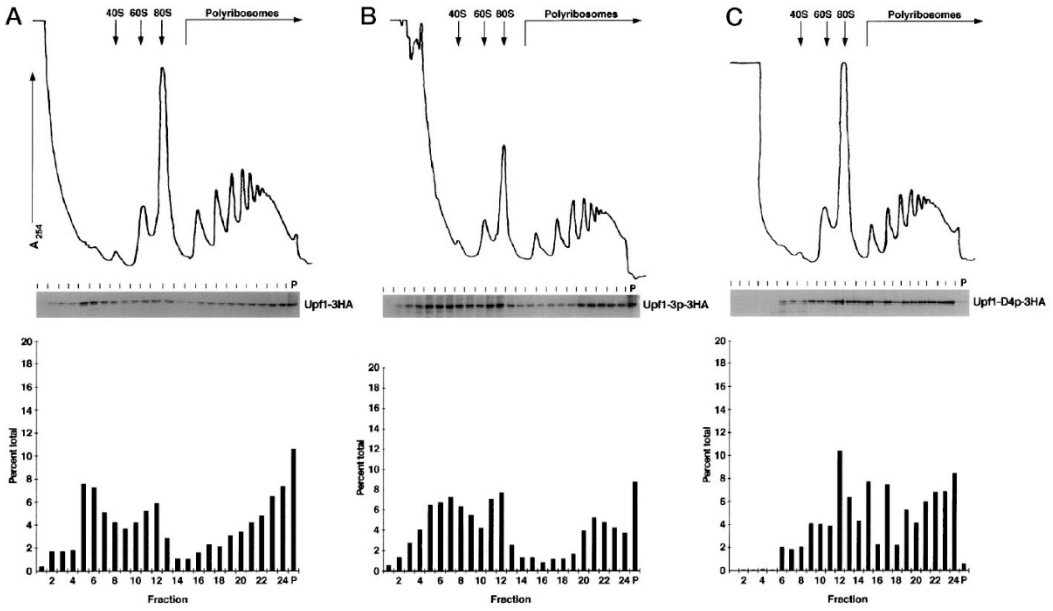

Figure 4. Distribution of the epitope-tagged proteins Upf1p-3HA, Upf1–3p-3HA, and Upf1-D4p-3HA in 7–47% sucrose gradients. Cell extracts were prepared from PLY102 [pRS314UPF1–3HA] (A), PLY102[pRS314upf1–3-3HA] (B), and PLY102[pRS314UPF1-D4–3HA] (C). The gradients were analyzed as described in Figure 2.

Distribution of Upf2p-3myc

Prior to these studies, it was not known whether Upf2p or Upf3p associate with polyribosomes in a manner resembling the demonstrated association for Upf1p (15). The distribution of Upf2p-3myc was analyzed in sucrose gradients using soluble lysates prepared from strain JDY8[pRS316UPF2–3myc] (Tables I and II), which contains wild-type *UPF1* and *UPF3* alleles (Fig. 5A). Upf2p-3myc was distributed throughout most of the gradient with two major peaks of accumulation corresponding to fractions containing ribosomal subunits and 80 S particles (fractions 7–13). The remainder was detected in heavier fractions containing polyribosomes (fractions 14–24).

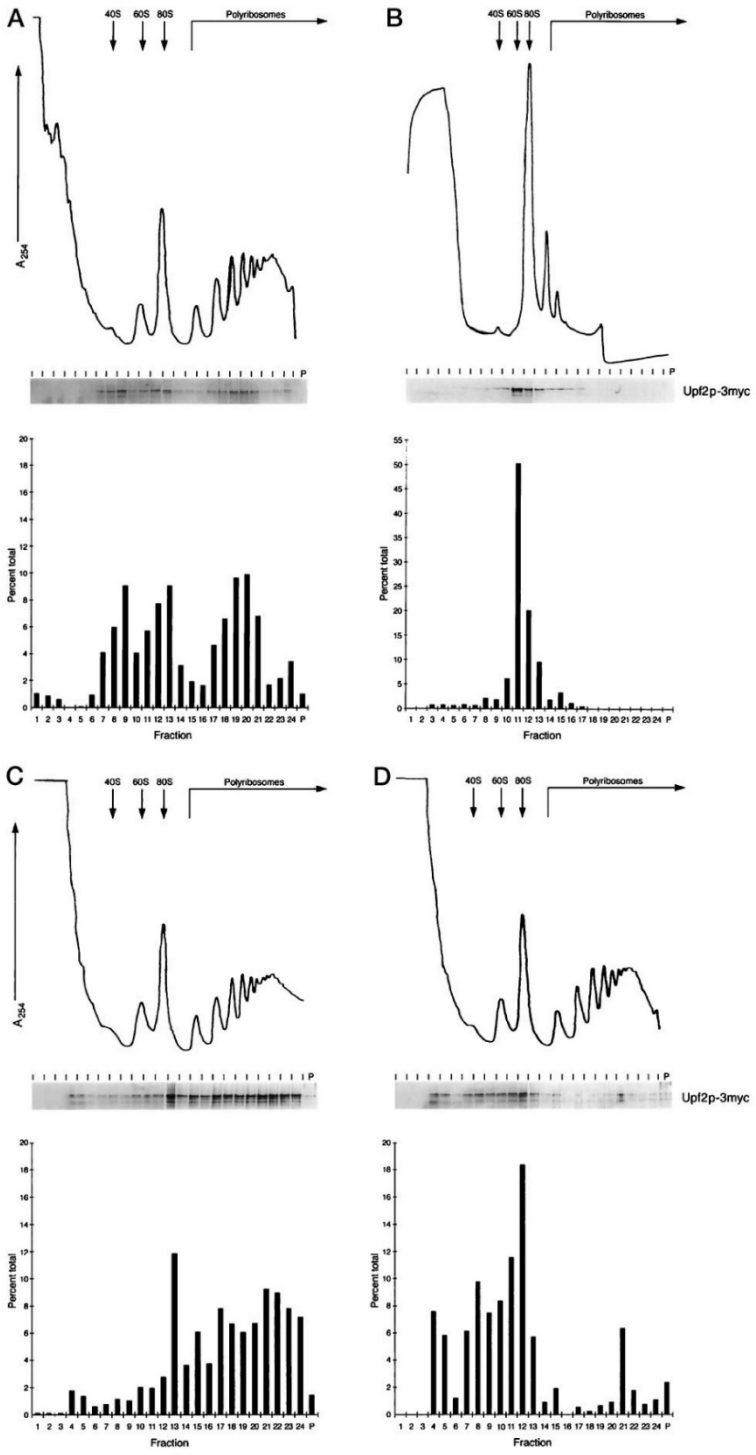

Figure 5. 7–47% sucrose density gradient fractionation of Upf2p-3myc in the presence or absence of a functional *UPF1* or *UPF3* gene. Cell extracts were prepared from strain JDY8-

[pRS316UPF2–3myc] (A), which carries functional versions of all three *UPF* genes, strain JDY8[pRS316UPF2–3myc] (B), pretreated with RNase A prior to fractionation, strain LRSY307[pRS316-UPF2–3myc, pLS74] (C), which carries a *UPF1* disruption, and strain LRSY307-[pRS316UPF2–3myc, pRS315UPF1] (D), which carries a *UPF3* disruption. The gradients were analyzed as described in Figure 2.

To determine whether codistribution of Upf2p-3myc with polyribosomes in the gradient reflects an association of the two, an experiment was performed using limited RNase A digestion of a lysate prior to fractionation. RNase digestion was shown previously to cause a collapse of the polyribosome profile into a single 80 S peak (15). When a soluble lysate prepared from strain JDY8[pRS316UPF2-3myc] was treated with RNase A prior to fractionation, the resulting optical density profile (A_{254}) collapsed into a major peak (fractions 10–13) corresponding to 80 S ribosomal particles (Fig. 5B). A coincident redistribution of UPF2p-3myc into fractions containing 80 S particles was also observed. This indicates that the distribution of Upf2p-3myc is dependent on the distribution of polyribosomes and suggests that the protein is associated with polyribosomes.

Next we tested whether the typical distribution of Upf2p-3myc requires the presence of Upf1p or Upf3p. To test the effect of disrupting *UPF1*, a soluble lysate was prepared from strain LRSY307[pRS316UPF2–3myc, pLS74] (Tables I and II). Compared with the profile in Fig. 5A, disruption of *UPF1* causes a decrease in the amount of Upf2p-3myc detected in fractions 7–13, which contain ribosomal subunits and 80 S particles (Fig. 5C). We found a corresponding increase in the amount detected in fractions 14–24, which contain polyribosomes. Assuming that the stability of Upf2p-3myc is unaffected in the absence of Upf1p, this result is indicative of a shift of the protein toward fractions containing polyribosomes.

To test the effect of disrupting *UPF3*, a soluble lysate was prepared from strain LRSY307[pRS316UPF2–3myc, pRS315-UPF1] (Tables I and II). Compared with the profile in Fig. 5A, disruption of *UPF3* drastically alters the profile (Fig. 5D). The majority of Upf2p-3myc was detected in fractions 4–13 with peak accumulation occurring in fractions 12, which is coincident with 80 S ribosomal particles. A significant amount of the protein was detected in fractions with densities lighter than 80 S particles. Only a minor amount of the protein was detected in fractions that contain polyribosomes (fractions 14–24). This result is indicative of a shift of Upf2p-3myc out of fractions containing polyribosomes in the absence of Upf3p.

Distribution of Upf3p-3HA

The distribution of Upf3p-3HA was analyzed in a manner similar to that described above for Upf2p-3myc. However, 12CA5 antibodies cross-react with a 51-kDa soluble yeast protein that migrates at a position similar to Upf3p-3HA on Western blots (not shown). The presence of the cross-reacting protein was not a problem in the detection of Upf1p-3HA because its larger size allowed for unambiguous identification. To distinguish between the cross-reacting protein and Upf3p-3HA, we performed a control experiment using a soluble lysate from strain LRSY203[pRS316], which lacks the *UPF3–3HA* gene (Tables I and II) (Fig. 6A). The cross-reacting protein was detected almost exclusively in the lightest fractions of

the gradient (fractions 1–3). In subsequent experiments, we regarded the protein detected in these fractions as being the cross-reacting protein rather than Upf3p-3HA.

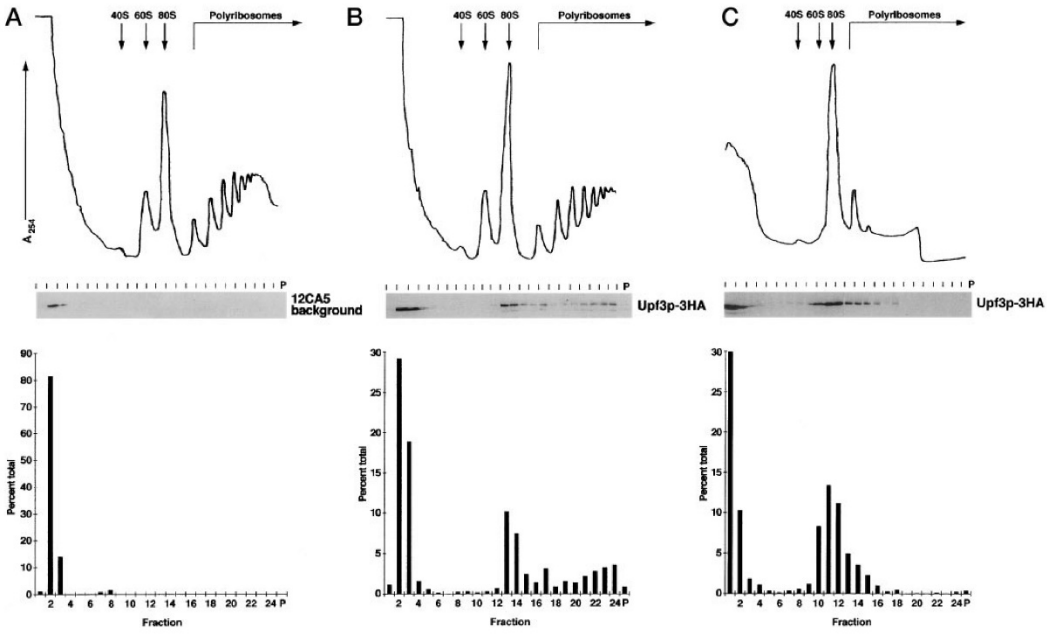

Figure 6. 7–47% sucrose density gradient fractionation of UPF3–3HA. Extracts were prepared from cells grown at 30°C using strains LRSY203[pRS316] (A), which lacks *UPF3–3HA*, strain LRSY203[pLS51] (B), which carries *UPF3–3HA*, and strain LRSY203[pLS51] (C) pretreated with RNase A prior to fractionation. The gradients were analyzed as described in the legend to Figure 2.

The distribution of Upf3p-3HA was analyzed in a sucrose gradient using a soluble lysate prepared from strain LRYS203[pLS51] (Tables I and II), which contains the *UPF3–3HA* gene and wild-type *UPF1* and *UPF2* genes (Fig. 6B). Upf3p-3HA was distributed in fractions 12–24 with peak accumulation occurring in fractions 13–14, which are coincident with 80 S ribosomal particles. A significant amount of Upf3p-3HA was detected in fractions containing polyribosomes (fractions 14–24). To determine whether the codistribution between Upf3p-3HA and polyribosomes is indicative of an association between the two, we performed limited RNase A digestion of a soluble lysate from strain LRSY203[pRLS51] (Fig. 6C). Compared with the distribution in Fig. 6B, the optical density profile (A_{254}) indicates that RNase A treatment causes polyribosomes to collapse into peak fractions 11 and 12, corresponding to 80 S ribosomal particles. Upf3p-3HA was redistributed into fractions 9–16 with a major peak corresponding to 80 S particles and a significant decrease in the amount of protein detected in fractions 14–24, which contain polyribosomes. Taken together, these results suggest that Upf3p-3HA is associated with polyribosomes.

Discussion

Mutations in each of the *UPF* genes suppress the same nonsense and frameshift mutations in a variety of genes and they have similar effects on the accumulation and decay of nonsense mRNAs (7, 8, 10–13). Previously it was shown that strains that are doubly null for pairwise combinations of the *UPF* genes have nonadditive effects on the turnover of nonsense mRNAs (10–13). In this paper, we show that isogenic strains carrying null mutations in all three of the *UPF* genes are viable and have nonadditive effects on the turnover of CYH2 pre-mRNA, which contains a premature termination codon in the inefficiently spliced intron causing it to be a target of NMD (27). These results suggest that the products of the *UPF* genes function in a common pathway leading to accelerated mRNA decay.

Recent evidence from two-hybrid studies suggests that Upf2p may form a bridge between Upf1p and Upf3p, allowing formation of a tripartite complex (17). However, data from the two-hybrid system provide little information on the stoichiometry of the interacting components. To begin addressing the stoichiometry of the Upf proteins, we determined the relative concentration of the epitope-tagged proteins Upf1p-3HA and Upf3p-3HA using quantitative Western blotting. Both proteins contain an identical sequence coding for three tandem copies of the HA epitope, with the tag located at the C terminus of Upf1p and the N terminus of Upf3p. The epitope-tagged proteins are expressed from their respective native promoters on the same single-copy *CEN* plasmid. Both proteins retain a level of function in NMD that is comparable with the level of function of their wild-type counterparts. From this, we infer that the presence of the epitope tags does not significantly destabilize either protein. The relative concentrations of the two epitope-tagged proteins should therefore provide a good approximation of the normal stoichiometry of wild-type Upf1p and Upf3p. Since both of the tagged proteins were detected on quantitative Western blots using fully denaturing conditions, the epitopes should be detected with equal efficiency.

Using this method and with these assumptions, we found that the overall concentration of epitope-tagged Upf3p was as much as 66-fold less than epitope-tagged Upf1p. If, as we expect, this reflects the relative *in vivo* ratio of the wild-type proteins, the concentrations of the two proteins deviate significantly from a 1:1 ratio, with Upf3p being the limiting factor. Other evidence supports a lower intracellular abundance for Upf3p. For example, a variety of epitope-tagged versions of Upf1p and Upf3p have been studied by immunofluorescence microscopy (15).[2] Upf3p consistently gives a much weaker fluorescent signal than Upf1p,[2] suggesting a large difference in the *in vivo* ratio of the two proteins. Although a tripartite complex may form, as suggested from two-hybrid analysis (17), the *in vivo* concentration of this putative complex may be relatively low and may form in the presence of an overall vast excess of Upf1p.

In addition to the stoichiometric limitation on complex formation, Upf1p and Upf3p exhibit major differences in intracellular distribution. The majority of soluble Upf1p, which accounts for about half of total Upf1p, is found in association with polyribosomes (15). Using indirect immunofluorescence and confocal microscopy, it was shown that Upf1p localizes throughout the cytoplasm with virtually no detectable protein found in the nu-

cleus. The distribution of Upf3p deviates significantly from that of Upf1p.[2] Indirect immunofluorescence reveals that Upf3p localizes both to the nucleus and to the cytoplasm with the greater proportion accumulating in the nucleus. Presumably, the nuclear fraction is not available for association with cytoplasmic polyribosomes. This is consistent with our results showing that about 15% of total Upf3p is soluble in polyribosome lysis buffer. Although most of soluble Upf3p codistributes with polyribosomes, this represents a minor fraction of total Upf3p. We assume that most of remainder may be located in the nucleus. We are currently studying the import and export of Upf3p across the nuclear envelope in an effort to determine how this protein or a complex it may be part of becomes available for interaction with cytoplasmic polyribosomes.

Upf1p was studied by examining the behavior of two epitope-tagged, mutant forms of the protein in sucrose gradients. One mutation, *upf1–3*, is located in a cysteine-rich domain that potentially binds zinc. The results of an allosuppression assay for NMD and an assay for accumulation of CHY2 pre-mRNA show that *upf1–3* severely impairs function. This same mutation causes reduced RNA helicase activity and impaired physical interaction with Upf2p (25). Using an epitope-tagged version of the mutant protein (Upf1–3p-3HA), we found that it distributed in a manner indistinguishable from Upf1p-3HA in sucrose gradients. Since the mutant protein associates normally with polyribosomes, it appears that helicase activity and interaction with Upf2p are not required in order for Upf1p to associate with polyribosomes.

The other mutation, called *UPF1-D4*, is located in a conserved residue in the RNA helicase domain. Previously, we studied the phenotypic effects of this mutation in strains that also carry a wild-type *UPF1* gene. We found that it confers dominant-negative inhibition of function of wild-type Upf1p (10). The strength of the inhibitory effect was dependent on the dosage of the *UPF1-D4* gene, with the strongest effect detected when a gene carrying the mutation was placed on a multicopy plasmid. Currently, the molecular basis for the dominant-negative phenotype is not understood.

To begin understanding the effects of this mutation, we examined the function of Upf1p-D4 in the absence of wild-type *UPF1*. Using this approach, it was possible to assess how the mutation affects function independently of its dominant-negative effects on wild-type Upf1p. We found that *UPF1-D4* causes a significant impairment of function when assayed by allosuppression. However, by examining the relative accumulation of CYH2 pre-mRNA, using RNA extracted from cells grown at 30°C, it appears that the mutant protein retains partial function. Upf1p-D4 presumably lacks function at 37°C, the temperature at which it exerts its dominant-negative effects. When we examined an epitope-tagged version of Upf1p-D4 in sucrose gradients, the mutation caused a modest shift of the protein toward heavier polyribosomes. This result indicates that the mutant protein retains its ability to associate with polyribosomes. In strains containing both mutant and wild-type proteins, it is therefore possible that the mutant protein competes with the wild-type protein for ribosome association. In addition, evidence from two-hybrid studies suggests that Upf1p homodimers may form, although the strength of the interaction was low (25). If homodimers form, then mutant/wild-type hybrids could form such that increasing the proportion of mutant subunits might lead to the observed dominant negative effects.

In this paper, we show that a portion of each of the three proteins found in soluble lysates codistributes in sucrose gradients in fractions containing polyribosomes. We find that each protein shifts along with polyribosomes into fractions containing 80 S ribosomal particles when lysates are treated with RNase A prior to fractionation. This indicates that the codistribution of the proteins most likely reflects association with polyribosomes. We studied these associations further by determining whether disruptions of the *UPF* genes affect the distribution of the Upf proteins in sucrose gradients. Upf1p appears to associate with polyribosomes by a mechanism that does not depend on the other two proteins, although a minor proportion of Upf1p was released from polyribosomes in the absence of Upf2p. The most dramatic effects were observed when the distribution of Upf2p was monitored in sucrose gradients using lysates from strains in which either the *UPF1* or *UPF3* gene was disrupted. Disruption of *UPF1* causes a shift in the distribution of Upf2p toward heavier polyribosomes. Disruption of *UPF3* had the opposite effect, causing a major redistribution of Upf2p into low-density fractions devoid of ribosomes.

The opposing effects resulting from disruption of *UPF1* or *UPF3* suggest that both proteins are needed to establish or maintain the normal equilibrium for association/dissociation of Upf2p with polyribosomes. The absence of Upf1p appears to promote association of Upf2p with polyribosomes, suggesting that the presence of Upf1p favors release of Upf2p from polyribosomes. The absence of Upf3p, which is present at limited concentrations, may cause the release of Upf2p from polyribosomes or may prevent association, suggesting that the presence of Upf3p is required for the association of Upf2p with polyribosomes.

These results are consistent with the notion derived from two-hybrid interactions that Upf2p could form a bridge between Upf1p and Upf3p (17). We envision a model in which Upf1p associates with polyribosomes by an independent mechanism using contacts that do not require the presence of the other two proteins. Upf2p may associate with polyribosomes through unique contacts separate from interaction with Upf1p but in a manner that may be influenced by Upf1p or Upf3p. This suggests that Upf1p and Upf2p may be docked or anchored to polyribosomes through separate mechanisms. A scheme for binding and release of Upf2p mediated by the other two proteins is consistent with the data and would still allow for physical interactions that might occur on polyribosomes.

Acknowledgments—We thank John Puziss and Phil Hieter for providing yeast strain YJP121 and plasmid pUZ178. We thank Leanne Olds for preparation of figures. This research was supported by the College of Agricultural and Life Sciences, University of Wisconsin (Madison, WI) Public Health Service Grant GM26217 (to M.R.C.), an Alberta Heritage Foundation for Medical Research supplemental research allowance, and a Natural Sciences and Engineering Research Council of Canada postdoctoral fellowship (to A.L.A.).

Notes

1. The abbreviations used are NMD, nonsense-mediated mRNA decay; HA, hemagglutinin; mAb, monoclonal antibody.
2. L. R. Schenkman, M. J. Lelivelt, R. Shirley, A. Ford, J. N. Dahlseid, and M. R. Culbertson, manuscript in preparation.

References

1. Green, L. L., and Dove, W. F. (1988) *J Mol Biol* 200, 321–328.
2. Laird-Offringa, I. A., Elfferich, P., and van der Eb, A. J. (1991) *Nucleic Acids Res.* 19, 2387–2394.
3. Paek, I., and Axel, R. (1987) *Mol. Cell. Biol.* 7, 1496–1507.
4. Decker, C. J., and Parker, R. (1993) *Genes & Dev.* 7, 1632–1643.
5. Beelman, C. A., Stevens, A., Caponigro, G., LaGrandeur, T. E., Hatfield, L., Fortner, D. M., and Parker, R. (1996) *Nature* 382, 642–646.
6. Larimer, F. W., Hsu, C. L., Maupin, M. K., and Stevens, A. (1992) *Gene* (*Amst.*) 120, 51–57.
7. Leeds, P., Peltz, S. W., Jacobson, A., and Culbertson, M. R. (1991) *Genes & Dev.* 5, 2303–2314.
8. Peltz, S. W., Brown, A. H., and Jacobson, A. (1993) *Mol. Cell. Biol.* 7, 1737–1754.
9. Muhlrad, D., and Parker, R. (1994) *Nature* 370, 578–581.
10. Leeds, P., Wood, J. M., Lee, B. S., and Culbertson, M. R. (1992) *Mol. Cell. Biol.* 12, 2165–2177.
11. Cui, Y., Hagan, K. W., Zhang, S., and Peltz, S. W. (1995) *Genes & Dev.* 9, 423–436.
12. He, F., and Jacobson, A. (1995) *Genes & Dev.* 9, 437–454.
13. Lee, B. S., and Culbertson, M. R. (1995) *Proc. Natl. Acad. Sci. U.S.A.* 92, 10354–10358.
14. Czaplinski, K., Weng, Y., Hagan, K. W., and Peltz, S. W. (1995) *RNA* 1, 610–623.
15. Atkin, A. L., Altamura, N., Leeds, P., and Culbertson, M. R. (1995) *Mol. Biol. Cell* 6, 611–625.
16. Fields, S., and Song, O. (1989) *Nature* 340, 245–246.
17. He, F., Brown, A. H., and Jacobson, A. (1997) *Mol. Cell. Biol.* 17, 1580–1594.
18. Rose, M. D., Winston, F., and Hieter, P. (eds.) (1990) *Methods in Yeast Genetics*, Cold Spring Harbor Laboratory, Cold Spring Harbor, NY.
19. Gietz, D., St. Jean, A., Woods, R. A., and Schiestl, R. H. (1992) *Nucleic Acids Res.* 20, 1425.
20. Grey, M., and Brendel, M. (1992) *Curr. Genet.* 22, 83–84.
21. Sambrook, J., Fritsch, E. F., and Maniatis, T. (1989) *Molecular Cloning: A Laboratory Manual*, Cold Spring Harbor Laboratory, Cold Spring Harbor, NY.
22. Lee, S. Y., and Rasheed, S. (1990) *BioTechniques* 9, 676–679.
23. Ausubel, F. M., Brent, R., Kingston, R. E., Moore, D. D., Seideman, J. G., Smith, J. A., and Struhl, K. (eds.) (1993) *Current Protocols in Molecular Biology*, Green Publishing Associates and Wiley-Interscience, New York.
24. Klessig, D. F., and Berry, J. O. (1983) *Plant Mol. Biol. Rep.* 1, 12–18.
25. Weng, Y., Czaplinski, K., and Peltz, S. W. (1996) *Mol. Cell. Biol.* 16, 5491–5506.
26. He, F., Peltz, S. W., Donahue, J. L., Rosbash, M., and Jacobson, A. (1993) *Proc. Natl. Acad. Sci. U.S.A.* 90(15), 7034–7038.
27. Kaufer, N. F., Fried, H. M., Schwindinger, W. F., Jasin, M., and Warner, J. R. (1983) *Nucleic Acids Res.* 11, 3123–3135.